Molecular Crystals and Liquid Crystals

Publication details, including instructions for authors and subscription information:
http://www.tandfonline.com/loi/gmcl20

Charge Mobility in Discotic Materials Studied by Pr-Trmc

John M. Warman [a] & Anick M. Van De Craats [a]

[a] Radiation Chemistry Department, IRI, Delft University of Technology, Mekelweg 15, Delft, 2629 JB, The Netherlands

Version of record first published: 18 Oct 2010

To cite this article: John M. Warman & Anick M. Van De Craats (2003): Charge Mobility in Discotic Materials Studied by Pr-Trmc, Molecular Crystals and Liquid Crystals, 396:1, 41-72

To link to this article: http://dx.doi.org/10.1080/15421400390213186

Mol. Cryst. Liq. Cryst., Vol. 396, pp. 41–72, 2003

ISSN: 1542-1406 print/1563-5287 online
DOI: 10.1080/15421400390213186

Taylor & Francis
Taylor & Francis Group

CHARGE MOBILITY IN DISCOTIC MATERIALS STUDIED BY PR-TRMC

*John M. Warman and Anick M. Van De Craats**
Radiation Chemistry Department, IRI, Delft University of Technology, Mekelweg 15, 2629 JB Delft, The Netherlands

The application of the pulse-radiolysis time-resolved microwave conductivity technique, "PR-TRMC", to the determination of intracolumnar charge carrier mobilities within mesomorphic discotic materials is described. A review is given of the mobility values obtained for the large variety of materials which have been studied since the first results were reported in 1989. This includes peripherally substituted derivatives of triphenylene, phthalocyanine, porphyrin and hexabenzo-coronene. The influences of temperature, morphology and variations in the primary molecular structure are demonstrated and discussed. Both the mesomorphic and conductive properties are shown to be dramatically influenced by subtle changes in the peripheral alkyl chain structure or the core-to-chain coupling element, in addition to changes in the nature of the aromatic core itself. Mobilities as high as 1 cm^2/Vs are found in crystalline solids, and well in excess of 0.1 cm^2/Vs in columnar, liquid crystalline phases; values which approach those for electrons and holes in organic single crystals. The PR-TRMC mobility values are in reasonable agreement with values determined by the time-of-flight method (TOF) for the mesophase of triphenylene derivatives; the only class of discotic compounds for which the TOF method has been applied with success. In addition to its more general applicability to a range of core structures, the PR-TRMC method has the advantage that it does not require homeotropic alignment of the sample and even polycrystalline materials can be studied. A disadvantage is that only the sum of the charge carrier mobilities is measured; the sign of the major carrier cannot therefore be determined.

Keywords: Discotic liquid crystals, charge mobility, microwave conductivity, pulse radiolysis, triphenylene, phathalocyanine, porphyrin, hexabenzocoronene

INTRODUCTION

In the PR-TRMC approach the material of interest is ionized by a nanosecond pulse of high-energy electrons from a Van de Graaff accelerator. This

*Present address: Netherlands Forensic Institute, Chemistry Department, PO Box 3110, 2280 GC Rijswijk, The Netherlands, E-mail: a.van.de.craats@nfi.minjus.nl

results in the creation of charge carriers with a uniform and known concentration on the order of micromolar. If the charge carriers formed are mobile this results in an increase in the conductivity of the sample which is monitored with nanosecond time-resolution as a transient decrease in the power of microwaves which propagate through the irradiated medium. A PR-TRMC conductivity transient has two characteristics; the magnitude at the end of the pulse, which is proportional to the product of the concentration of carriers formed and their mobility, and the decay after the pulse, which provides information on the subsequent recombination and/or trapping of the mobile charge carriers. A simple schematic representation of the technique is shown in Figure 1. A detailed description of the apparatus used and the method of data analysis is given in the experimental section and in separate publications[1–4].

In the first reports of the application of the technique to discotic materials the main interest was in the after-pulse decay of the conductivity rather than the absolute magnitude[5,6]. The timescale of the decay was found to increase exponentially with increasing length of the mesogenic alkyl chains in a series of octa-*n*-alkoxy-substituted phthalocyanines, varying from a few hundred nanoseconds for hexyl to milliseconds for octadecyl[7,8]. This was attributed to the fact that the positive and negative charge carriers being observed were on separate columnar stacks and could

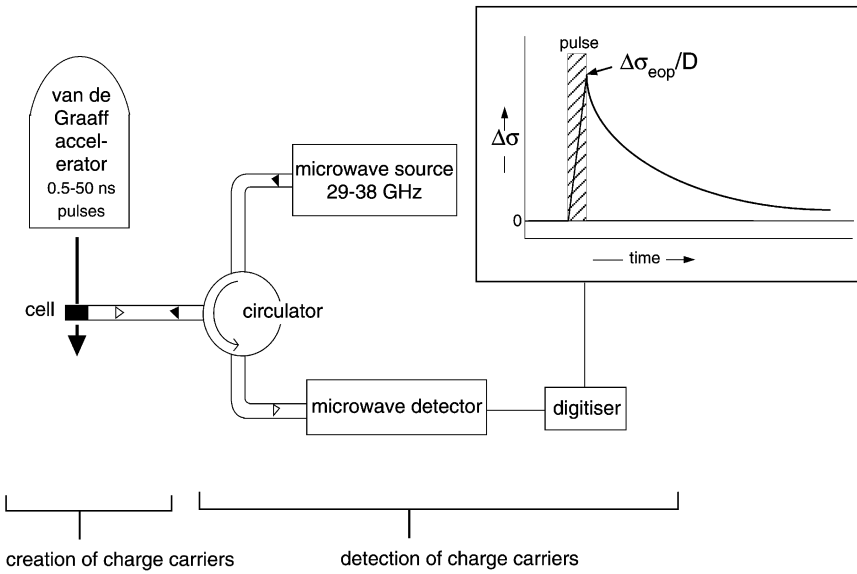

FIGURE 1 A much simplified schematic of the PR-TRMC equipment.

only recombine via intercolumnar tunneling through the saturated hydrocarbon mantle surrounding the stacked aromatic cores.

Attention has been focussed in more recent years on the one-dimensional mobility of charge carriers within the columnar stacks which can be derived from the end-of-pulse conductivity. This shift of attention was to a large extent in response to a growing interest in discotic compounds as potential one-dimensional semiconductor materials in device applications such as photovoltaic cells, light-emitting diodes, and field-effect transistors.

Initial rough estimates of mobility values derived from PR-TRMC measurements on phthalocyanine and porphyrin derivatives indicated that these could be well in excess of $0.1\,cm^2/Vs$[5–9]. At that time, this was orders of magnitude larger than estimates for discotic materials based on other methods of investigation. The mobility was furthermore found to *decrease* significantly on going from the crystalline solid to the liquid crystalline mesophase of phthalocyanine and porphyrin derivatives as shown in Figures 2 and 3[9,10]. This result was controversial at the time since the currently held belief was that the more favourable π-π overlap in the horizontally-stacked D_h phase should result in a *higher* charge mobility than in the K phase with its tilted stacking of the aromatic cores. The results on the porphyrin derivatives were of particular importance since their clearing points were within the temperature range of the experiments. It was possible therefore to demonstrate that the substantial decrease in mobility on going from the K to the D_h phase, was followed by an even more dramatic decrease at the transition to the isotropic liquid as shown in Figure 3. This provided the first direct evidence that columnar self-assembly in the liquid crystalline phase of discotic materials results in charge mobilities much larger than possible via molecular diffusion alone.

On the basis of a model for the formation of the relatively long-lived, mobile charge carriers in pulse-irradiated discotic materials, a quantitative method of estimating mobilities from the end-of-pulse PR-TRMC transients was subsequently derived[3,7]. This confirmed the previous estimates of values close to $0.1\,cm^2/Vs$ or higher for discotic derivatives of porphyrin and phthalocyanine. At approximately the same time the first non-dispersive time-of-flight measurements on triphenylene derivatives were reported[11,12]. It was therefore decided to carry out a comparative study of results obtained using PR-TRMC with TOF measurements on the classic discotic compound hexakis-hexylthiotriphenylene (HHTT) [13]. As can be seen in Figure 4, the agreement between the two techniques was found to be extremely good for both the helical and the columnar hexagonal phases. By combining the results obtained using both techniques, a complete description of the change in the mobility by more than three orders of magnitude in going from the K phase ($\mu \approx 0.3\,cm^2/Vs$) , via the H and D_h mesophases, to the isotropic liquid ($\mu \approx 0.0001\,cm^2/Vs$) could be made.

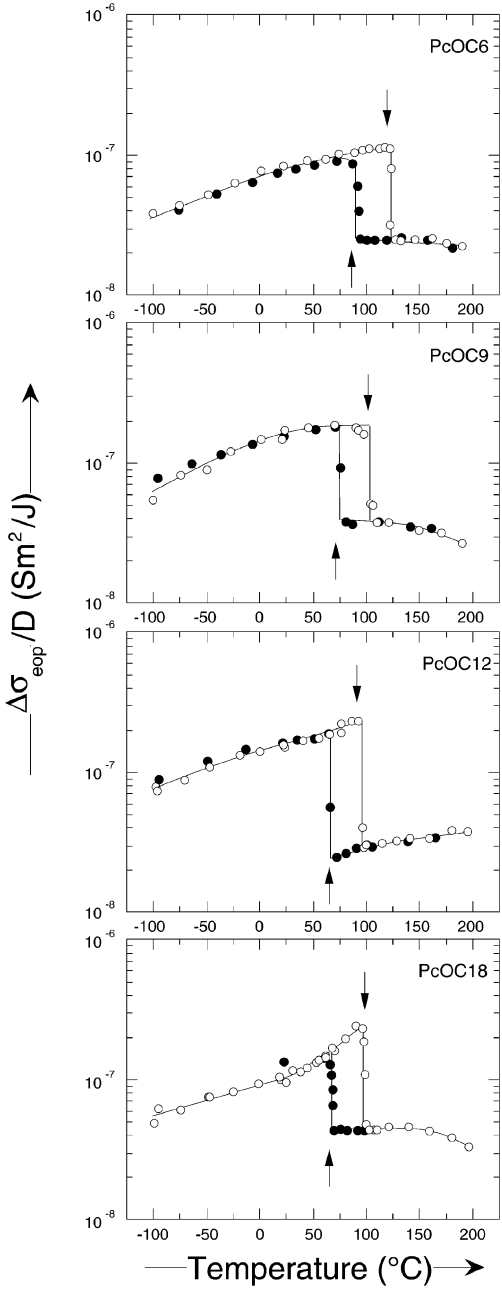

FIGURE 2 The temperature dependence of the dose-normalized radiation-induced conductivity for octa-*n*-alkoxy substituted phthalocyanine derivatives on heating (open circles) and cooling (filled circles) for $n = 6$, 9, 12, and 18. The vertical arrows indicate the K-D and D-K transition temperatures as determined by DSC. From reference [1].

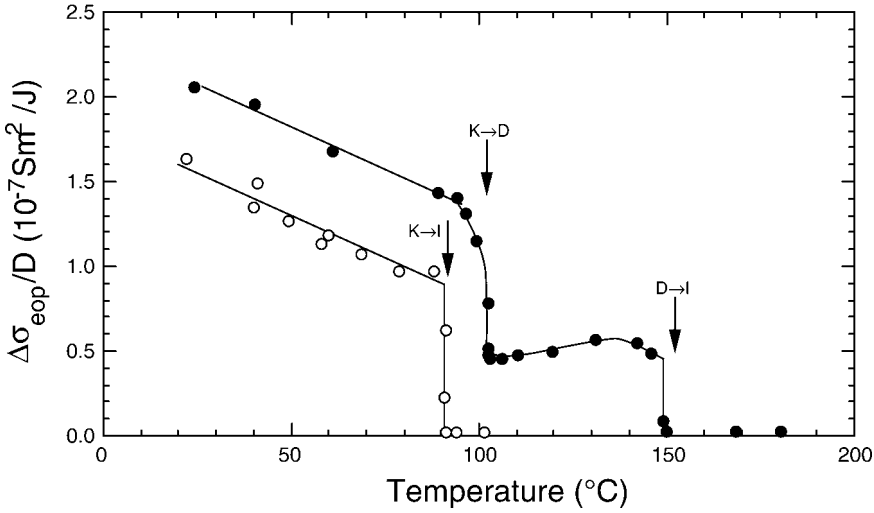

FIGURE 3 The temperature dependence on heating of the dose-normalized radiation-induced conductivity of octa-nonoxyethyl metal-free (open circles) and zinc (filled circles) porphyrin derivatives. The phase transition temperatures as determined by DSC are indicated by vertical arrows. From reference [1].

The good agreement confirmed the proposition that the mobility determined by PR-TRMC corresponds to that in well-organised, columnar domains within the bulk materials studied and as such represents the highest DC mobility that should be achievable in a homeotropically well-organised sample.

In the present paper we have compiled the mobility values obtained using the PR-TRMC technique for a variety of discotic materials based on mesomorphic derivatives of (hetero)aromatic cores of triphenylene, phthalocyanine, porphyrin and hexabenzocoronene. A detailed description of the experimental and data analysis procedures is given and some general conclusions about the factors affecting charge transport in discotic materials based on the results obtained are summarised.

EXPERIMENTAL

Sample Preparation

The discotic compounds investigated were usually received as freshly precipitated, polycrystalline solids. Occasionally, the materials were liquid crystalline even at room temperature and these were characterised by a sticky, malleable or plastic texture. In the majority of cases the samples

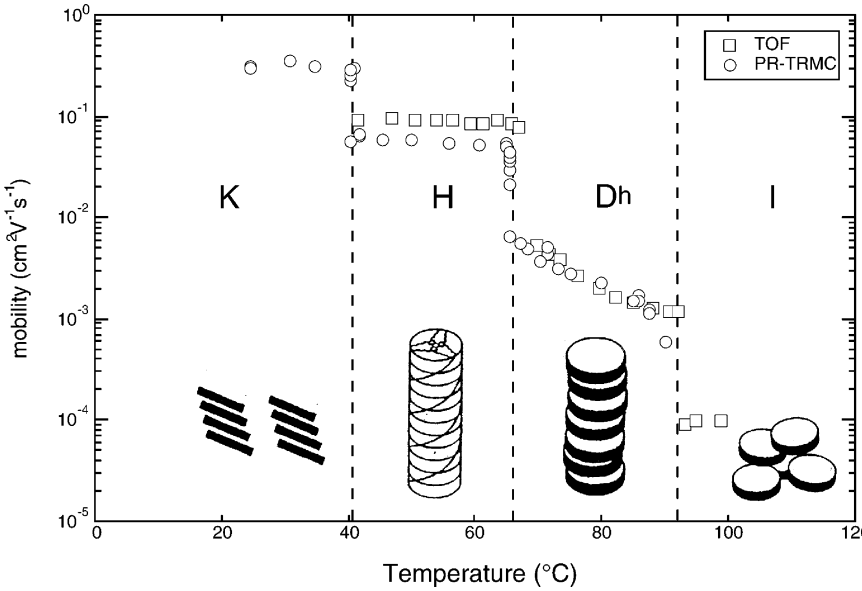

FIGURE 4 A comparison of the temperature dependence of the charge mobility determined by PR-TRMC with the hole mobility determined by TOF on cooling hexakis(hexylthio)-triphenylene from the isotropic liquid phase. The phase transition temperatures are indicated by the vertical dashed lines. From reference [2].

were accompanied by measurements of their mesomorphic and structural properties carried out at the source by differential scanning calorimetry (DSC), polarization microscopy (POMIC), and small-angle X-ray diffraction (SAXS). In this regard it is important to note that PR-TRMC measurements are usually carried out starting with the material as received with no prior thermal treatment. The initial temperature trajectory corresponds therefore to the *first* heating run on the pristine material. Since the initial structure of freshly-precipitated discotic materials is quite often not retrieved on cooling from higher temperature phases, it is important, for comparative purposes, that the complementary structural information is available for the *pristine material* at room temperature and for the *first* heating trajectory.

Samples are prepared for PR-TRMC measurements by compressing the material, into a rectangular cell using a close-fitting PTFE rod. The cell consists of a 14 mm long piece of Ka-band (26.5–42 GHz) copper waveguide with an internal cross section of $3.55 \times 7.1\,\text{mm}^2$ which is closed at one end by a metal plate ("short-circuit") and flanged at the other end for connection to the microwave circuitry, see Figure 5. For reasons of chemical purity the cell is gold-plated using Atomex solution (Engelhard Industries).

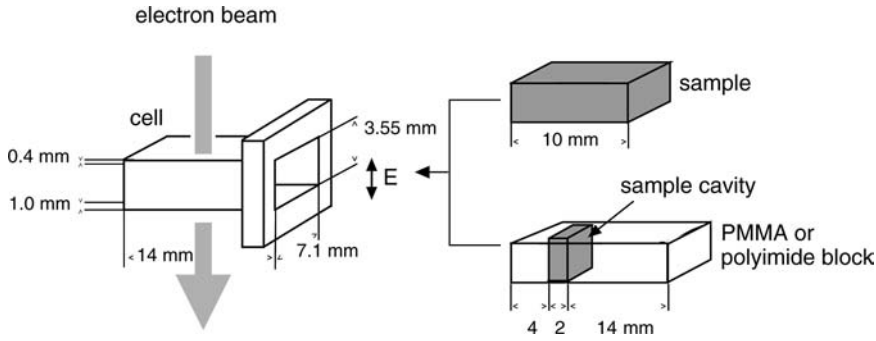

FIGURE 5 The waveguide cell used for PR-TRMC measurements on bulk solid materials. The cell can be either completely filled to a length of *ca* 10 mm (200 mg) or can be filled with a PMMA or polyimide block with a small sample cavity (*ca* 25 mg).

The length (*ca* 10 mm) and weight (*ca* 200 mg) of the sample are accurately measured and used to calculate the fraction of the sample volume actually consisting of bulk solid based on the known density of the solid or, if unknown, assuming the density to be close to 1 g/cm^3. This "fill-factor", F, which is usually between 0.6 and 0.8, is used to correct the radiation-induced conductivity for the fact that the sample volume is not completely filled.

When less than *ca* 200 mg of the material is available, approximately 25 mg is compressed into a cavity of dimensions $6 \times 3 \times 2$ mm^3 in a PMMA or polyimide block as shown in Figure 5. The blocks have outer cross-sectional dimensions slightly smaller than the inner dimensions of the waveguide cell into which they are inserted after filling. The block materials were chosen on the basis of their own extremely small radiation-induced conductivity.

The filled cell is attached to the waveguide circuitry and is enclosed in a cryostat capable of covering a temperature range from −100 to +200°C. The temperature is regulated by a thermocouple in contact with the cell. When a PMMA block is used the maximum temperature is limited to 120°C.

Pulse-Radiolysis

The cell is irradiated with a single pulse of 3 MeV electrons from a Van de Graaff accelerator. The pulses are close to square with rise and fall times of *ca* 100 ps and a width which can be varied from 0.5 to 50 ns. The beam current can also be varied but is usually kept close to 4 A, giving a range of integrated beam charge per pulse, Q, from 2 to 200 nC depending on the pulse-width used. The actual value of Q is routinely measured accurately

during the course of a series of measurements by deflecting the beam onto a target connected to an electrometer. The pulse-to-pulse reproducibility is usually better than 2%.

The gaussian half-width of the beam cross-section is larger than the lateral dimensions of the sample [4] and the penetration depth of 3 MeV electrons in materials of density 1 g/cm^3 is *ca* 15 mm, i.e. much larger than the sample thickness of 3.5 mm. Energy deposition and ionization within the sample is therefore close to uniform. The dose inside the cell per unit beam charge, D_v/Q, is determined accurately using Far West Technology-92 radiochromic dosimeter films and was close to 1 kJ/m^3/nC. For a beam current of 4 A and the range of pulse lengths available, the total dose in a single pulse can therefore be varied from 2 to 200 kJ/m^3. It is worth emphasising that for high-energy electrons the dose per unit volume and the penetration depth are dependent only on the electron density of the material irradiated and are completely insensitive to its color or morphology. For the same pulse conditions, the energy deposited per unit volume is therefore very similar for all organic materials.

If E_p is the average energy in electron volts required per ionization event, then the total concentration of charge carrier pairs formed within a single pulse, $N_p(0)$, is given by

$$N_p(0) = D_v/eE_p \tag{1}$$

with e the value of the elementary charge (1.6×10^{-19}). For organic materials E_p is close to 20 eV (see below). The above dose range corresponds therefore to a range of charge carrier pair concentrations from *ca* 6 to 600×10^{20} m^{-3} (1 to 100 μmole/litre, or approximately 1 to 100 ionization events per million molecules for the type of materials studied here).

The value of E_p for high-energy radiation, has been found to be given to a good approximation by the (semi)empirical expression derived by Alig *et al* [14]

$$E_p \approx 2.73 \times E_I + 0.5 \tag{2}$$

In (2), E_I is the minimum energy required for ionization, i.e. the ionization potential for molecular materials or the bandgap in the case of semiconductor materials. Perhaps surprisingly, (2) is found to be quite universal, providing reasonable estimates of E_p for materials varying from low bandgap inorganic semiconductors with E_I as low as 1 eV, to organic hydrocarbon liquids for which E_I is closer to 10 eV. If a reasonably accurate estimate of E_I can be made, then (2) is expected to give a value of E_p which is good to within ± 20%. We emphasise that the concentration of charge carrier pairs calculated on the basis of (1) using the value of E_p derived from (2) yields the concentration of *initial* ionization events and hence the

maximum concentration of primary charge carrier pairs that could be present at the end of the pulse, if no decay has occurred during the pulse via (geminate) recombination and/or trapping.

If a medium consists of different molecular components, the fraction of the total energy deposited initially in component X is proportional to its fractional contribution to the electron density of the medium, $Z_x/\Sigma(Z_x)$. If the components differ in their E_p values, the average value of E_p required to calculate the total concentration of ionization events is given by,

$$\langle Ep \rangle = \Sigma(Z_x)/\Sigma(Z/E_p)_x \tag{3}$$

For example for discotic materials the values of E_I for the aromatic core and the aliphatic hydrocarbon mantle would be expected to be somewhat different; *ca* 8 eV ($E_p = 22$ eV) for the former and closer to 6 eV ($E_p = 17$ eV) for the latter. For equal contributions to the electron density this would result in an average value of $\langle E_p \rangle = 19$ eV.

Time-Resolved Microwave Conductivity

Any change occurring in the conductivity of the sample on pulse-radiolysis is monitored as a change in the microwave power reflected by the sample cell. A simple schematic drawing is shown in Figure 1; more details are to be found in previous publications [1–4]. Microwaves are generated by a Gunn oscillator with a tunable frequency range from 27 to 38 GHz and an average power level of *ca* 100 mW. The microwaves are transmitted via a circulator to the sample cell where they propagate through the sample and are reflected at the end of the cell by the metal short circuit. The power level of 100 mW corresponds to a maximum electric field strength in the sample of *ca* 10 V/cm.The reflected microwaves are directed by the circulator to one of two detectors which monitor the microwave power. One of these is a slow-response linear power meter for measuring the absolute microwave power and for calibration of the other detector which is a fast time-response (*ca* 1 ns) Schottky barrier diode (Alpha Industries 1N53B).

The output of the 1N53B diode is connected to a cascade of home-built impedance matching amplifiers (IMA) and a video amplifier of the Comlinear type CLC 100. The low-noise IMA has a frequency range of 10 Hz to 1 GHz and consists of two FET's of type ATF 21186 with a total amplification factor of 3. The GLC 100 has a frequency range from DC to 0.5 GHz and an amplification factor of 10. The amplifier output can be fed into either a Tektronix SCD 100 or TDS 680B digital oscilloscope for registration of transients on a linear time-base with an overall response time of *ca* 1 ns. For longer times after the pulse a tandem combination of a Tektronix 2205

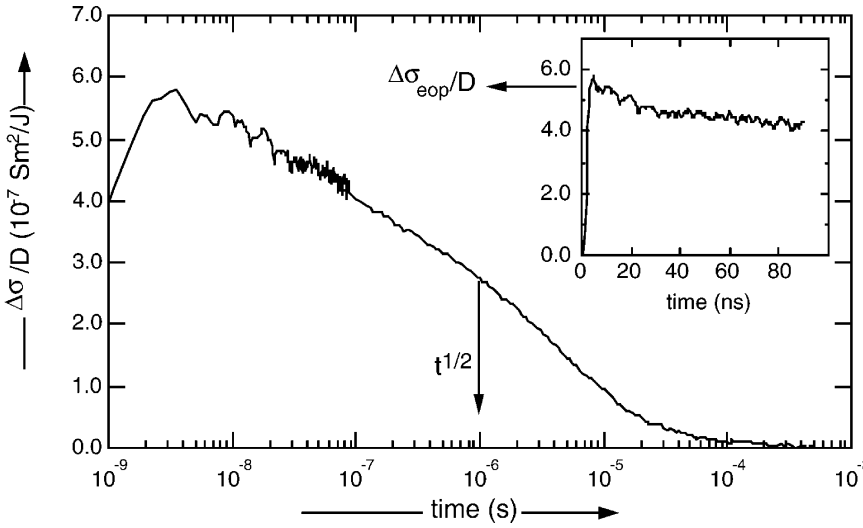

FIGURE 6 Conductivity transients obtained on 2 nanosecond pulsed irradiation of hexakis(*n*-tetradecyl)hexa-*peri*-benzocoronene (HBC-C14) in the crystalline solid phase at 55°C. In the inset a transient is shown as monitored on a linear timescale using the fast digitizer option. In the main figure the same transient is shown together with a transient taken using the digitizer combination capable of monitoring the conductivity from *ca* 10 ns to 10 ms using a logarithmic timescale. In both cases only a single pulse was used. From reference [2].

oscilloscope with a 7A13 plug-in and a Sony/Tektronix RTD 710 digitizer is used. This allows transients to be monitored from 10 ns to 10 ms on a pseudo-logarithmic time-base using a single pulse from the accelerator with however reduced time-resolution in the nanosecond range. Conductivity transients obtained using the linear and logarithmic timescale capabilities are shown in Figure 6 for a hexabenzocoronene derivative.

Apart from the digitizers, all active electronic components are contained in sheet-metal Faraday cages with special high-frequency EMI filtering devices for ventillation, power supply, and signal transmission. Only with such precautions can the high sensitivity of detection necessary be achieved. The noise level on the CW microwave power level on a nanosecond timescale is *ca* 0.01%. The signal to noise sensitivity can be improved by averaging up to 32 individual transients.

Data Analysis

In the present study only changes in the real component of the microwave conductivity (the imaginary or dielectric loss component of the

permittivity) are measured. The change in reflected power, $\Delta P_R/P_R$ is directly related to the radiation-induced change in the conductivity of the sample, $\Delta\sigma$, for relatively small changes by,

$$\Delta P_R/P_R = -AF\Delta\sigma \tag{5}$$

with F the fill factor and A the sensitivity parameter. A is a sinusoidally varying function of the microwave frequency due to interference effects resulting from the similarity between the dimensions of the sample and the wavelength of the probing microwaves (*ca* 10 mm in air). The value of A can be calculated on the basis of the known length of the sample and its "effective" dielectric constant [15,16]. TRMC transients are routinely taken at several frequencies within the available range of 27 to 38 GHz in order to increase the accuracy of the value of $\Delta\sigma$ determined. Typical frequency scans of end-of-pulse conductivity signals together with a calculated fit are shown in Figure 7. The oscillatory form of such scans is determined by the value of the effective dielectric constant of the medium and the absolute magnitude is determined by the value of the conductivity change.

The conductivity change at any time during or after the ionizing pulse is related to the concentration, N_i, and mobility, μ_i, of all charge carriers present at that time according to

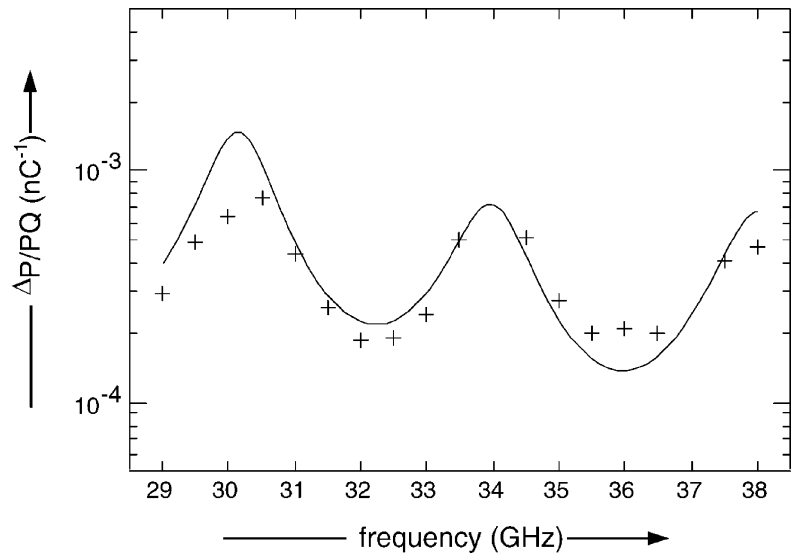

FIGURE 7 The frequency dependence of the absorbed microwave power per unit beam charge for a 2 ns pulse-irradiated sample of hexakis(*n*-tetradecyl)hexa-*peri*-benzocoronene (HBC-C14) in a polyimide container. The full-line fit to the data was calculated for a dielectric constant of 2.8. From reference [2].

$$\Delta\sigma(t) = e\Sigma[N_i(t)\mu_i] \tag{6}$$

For a pair of charge carriers with mobilities $\mu(-)$ and $\mu(+)$, the conductivity change at the end of a pulse will be given by,

$$\Delta\sigma_{eop} = eN_p(0)W_{eop}[\mu(-) + \mu(+)] \tag{7}$$

$$= eN_p(0)W_{eop}\Sigma\mu \tag{8}$$

W_{eop} in (7) and (8) is the pair survival probability, i.e. the fraction of initially formed charge carrier pairs that have *not* undergone rapid (geminate) recombination within the pulse. Substituting for $N_p(0)$ from (2) in (8) and rearranging results in the following expression for $\Sigma\mu$ in terms of the experimentally measureable parameter $[\Delta\sigma_{eop}/D_v]$,

$$\Sigma\mu = [\Delta\sigma_{eop}/D_v]E_p/W_{eop} \tag{9}$$

Since the maximum value of W_{eop} is unity, a minimum value of the sum of the mobilities of the charge carriers can be determined from the radiation-induced conductivity using (10).

$$\Sigma\mu_{min} = [\Delta\sigma_{eop}/D_v]E_p \tag{10}$$

Unfortunately, the separate mobility values of the positive and negative charge carriers cannot be determined using the present technique for bulk solids.

Some time ago a model was proposed on the basis of which W_{eop} was estimated for discotic materials [1,3,7]. In this model charge carrier pairs formed initially on the same stack of aromatic cores are assumed to undergo rapid, subnanosecond intracolumnar recombination. The electrons and holes of pairs formed within the saturated hydrocarbon mantle can diffuse to different columnar stacks in competition with their geminate recombination within the mantle. In this way the electron and hole of a pair can become localized on separate stacks with a barrier towards recombination provided by the intervening saturated hydrocarbon medium. In order to explain the conductivity observed the charge carriers must remain highly mobile even when "localized" on the aromatic cores. Strong evidence for this model was provided by the exponential dependence on the length of the alkyl chains found for the decay time of the conductivity in peripherally alkoxy-substituted phthalocyanines[5–8].

According to the above model, which is illustrated in Figure 8, the value of E_p is taken to be that for saturated hydrocarbons, i.e. *ca* 25 eV [17–19]. The value of W_{eop} is calculated from the product of the fraction of energy

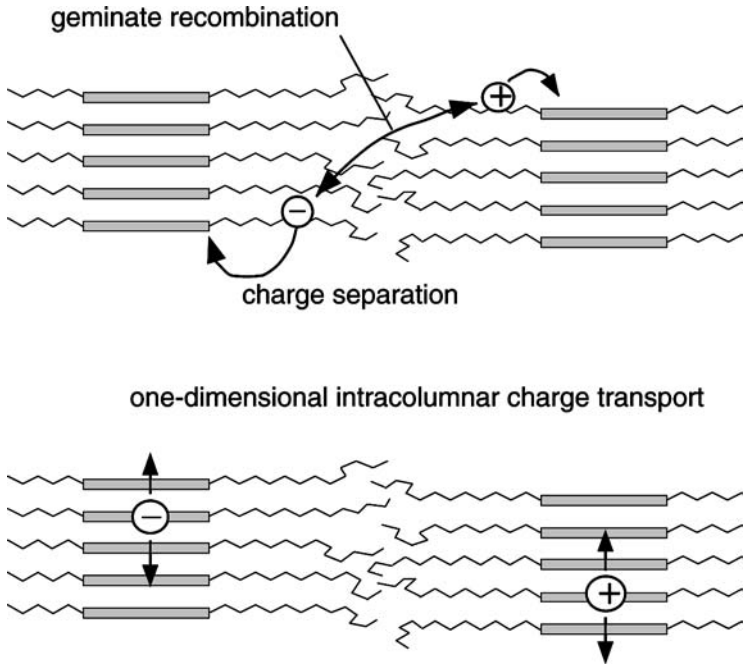

FIGURE 8 Schematic representations of the charge separation process following pulsed ionization which leads to the formation of long-lived, mobile charge carriers on separate columns in discotic materials. From reference [2].

absorbed in the saturated hydrocarbon component of the compound, $Z_{HC}/\Sigma Z_X$, and the probability of capture of electrons and holes by the aromatic cores in competition with their geminate recombination within the mantle, W_s. The value of W_s is estimated using the WAS charge scavenging equation,

$$W_s \approx 1/(1 + (\alpha[S])^{-1/2}) \tag{12}$$

taking for α a value of 10 L/mole, as found for electron scavenging in saturated hydrocarbon liquids [20]. The one-dimensional intracolumnar mobility is then calculated using (13).

$$\Sigma\mu_{1D} = 3E_p[\Delta\sigma_{eop}/D_v]/(W_s[Z_{HC}/\Sigma Z_x]) \tag{13}$$

The factor of 3 in (13) takes into account the fact that the organised columnar domains within a bulk sample are randomly orientated. The overall value of the parameter $W_{eop} = W_s[Z_{HC}/\Sigma Z_X]$ lies within the range 0.3 to 0.6 for all of the discotic materials studied.

RESULTS AND DISCUSSION

As pointed out in the introduction, it is the purpose of the present article to provide a compilation of the charge mobility measurements which have been made on discotic compounds using the PR-TRMC technique. Results for peripherally-functionalised derivatives of triphenylene, phthalocyanine, porphyrin and hexabenzocoronene are first presented separately, prior to giving some general conclusions which can be drawn about the various physical, chemical, and morphological parameters which influence charge transport in discotic materials.

Triphenylenes

Liquid crystalline triphenylenes have been the subject of many previous charge transport studies by others, [11,12,21–29] mainly because of their ease of processability and low clearing points. This makes it possible to achieve homeotropic alignment of the columns with respect to the electrode surfaces which is necessary for DC conductivity and time-of-flight (TOF) measurements. One of the most important conclusions from these studies is that charge transport is highly anisotropic with up to 3 orders of magnitude higher conductivity in the direction of the columnar stacks [25].

The molecular structures and pseudonyms of the triphenylene derivatives which have been studied by PR-TRMC are shown in Figure 9. In addition to the monomeric alkoxy- and alkylthio-substituted compounds two dimeric butoxy-substituted compounds joined by alkyl-chain bridging units have been investigated. All of the compounds, when freshly precipitated, are crystalline solids which on heating display a transition to a high-temperature liquid crystalline phase in which the aromatic cores are horizontally stacked in columns with a cofacial distance of close to 3.6 Å.

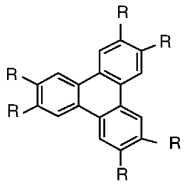

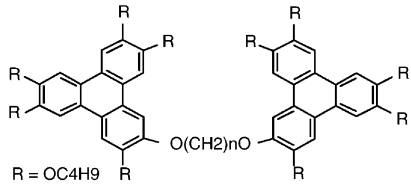

H6ST (= HHTT) R = SC6H13
H8ST R = SC8H17
H10ST R = SC10H21

H4OT R = OC4H9
H5OT R = OC5H11
H6OT R = OC6H13

T2-s10 n = 10
T2-s12 n = 12

FIGURE 9 Molecular structures and pseudonyms of the triphenylene dervatives investigated.

For all but the three butoxy-derivatives this phase is the well-known hexagonally-packed D_h phase first demonstrated by Chandrasekhar [30]. A more rigid mesophase is claimed for H4OT and the dimeric compounds[31–34]. In this so-called "plastic" liquid crystalline, D_p phase the lateral and longitudinal displacements of the molecules are thought to be restricted [31]. All of the compounds become isotropic liquids for temperatures well below 200°C.

The temperature dependences of $\Sigma\mu_{1D}$ are shown for the monomeric alkoxy and alkylthio derivatives in Figures 10 and 11 respectively. For all but the butoxy compound an abrupt decrease in mobility is observed on entering a higher temperature phase on heating. In the case of the transition to the isotropic liquid the mobilities decreased to a level which was too low to measure within the signal-to-noise limitations of the PR-TRMC technique. As shown by the TOF results in Figure 4 in the introduction, the mobility in the isotropic phase is in fact more than an order of magnitude lower than even the lowest value in the immediately preceding mesophase.

On cooling the mobility values for the different phases are recovered within a factor of approximately 2. A substantial hysteresis, of as much as *ca* 30°C for H10ST, is however apparent for all transitions apart from at the clearing point. The two separate liquid crystalline phases for H6ST (HHTT) have more extended temperature ranges during the cooling run which was therefore used for comparison with the TOF data in Figure 4.

From the heating and cooling runs for the butoxy derivative it is apparent that the mobility in the high temperature mesophase is actually higher than for the crystalline solid. This anomalous behaviour is also found for the two dimers and would appear to be a property unique to this more rigid, D_p phase. This will be discussed further below when the temperature dependence of the dimer results are compared with TOF data.

Mobility values found in the different phases of all of the triphenylene derivatives studied are listed in Table I. For the K-phases the mobility values of *ca* 0.2 cm^2/Vs for the alkylthio compounds are seen to be considerably larger than for the alkoxy derivatives which lie within the range 0.006 to 0.03 cm^2/Vs. At present we cannot decide whether this difference is due to structural differences in the geometrical relationship or the electronic coupling between neighbouring cores induced by the different coupling units. Perhaps it is a combination of both. This large difference between the alkylthio and alkoxy derivatives is no longer apparent in the D_h phase for which all compounds have mobilities lying within the range 0.002 to 0.02 cm^2/Vs. This is probably due to the fact that thermally-induced structural disorder in the mesophase is the controlling factor in charge transport rather than the electronic coupling between the triphenylene units as in the rigid crystalline solids.

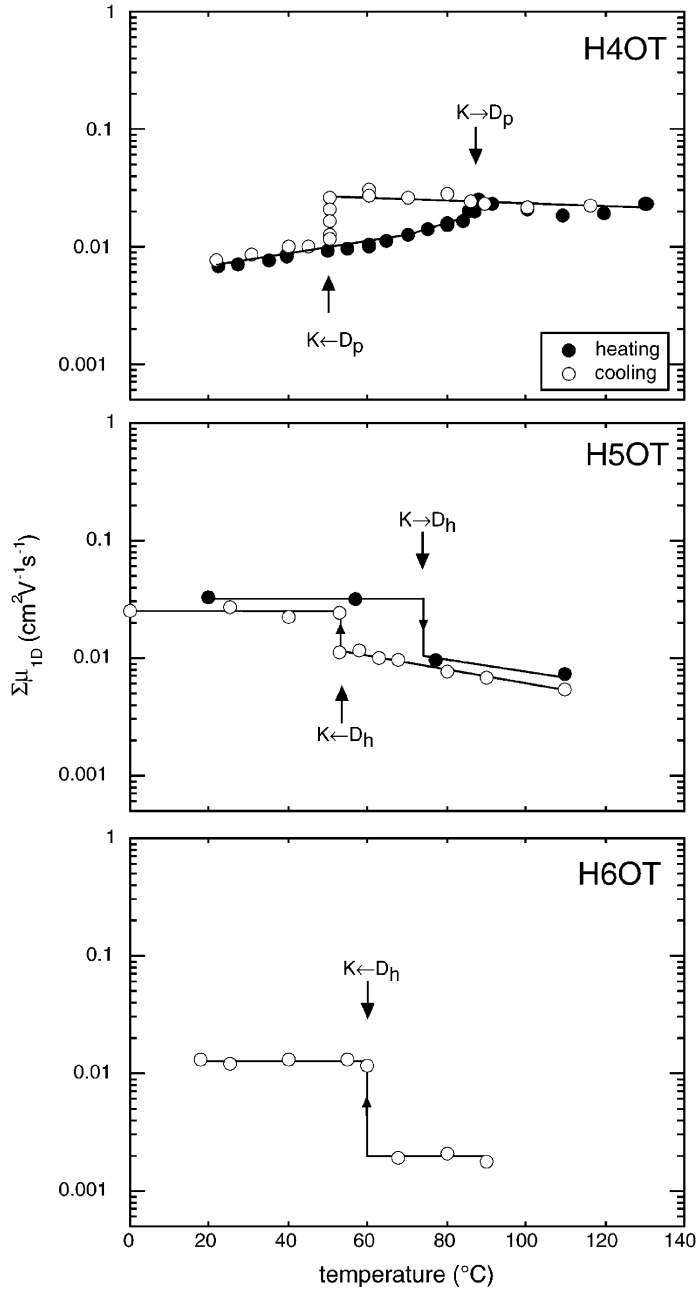

FIGURE 10 The temperature dependences of the intracolumnar charge mobility for hexakis(alkoxy)-triphenylenes on first heating (filled circles) and cooling (open circles). The phase transition temperatures as determined by DSC are indicated by vertical arrows. From reference [2].

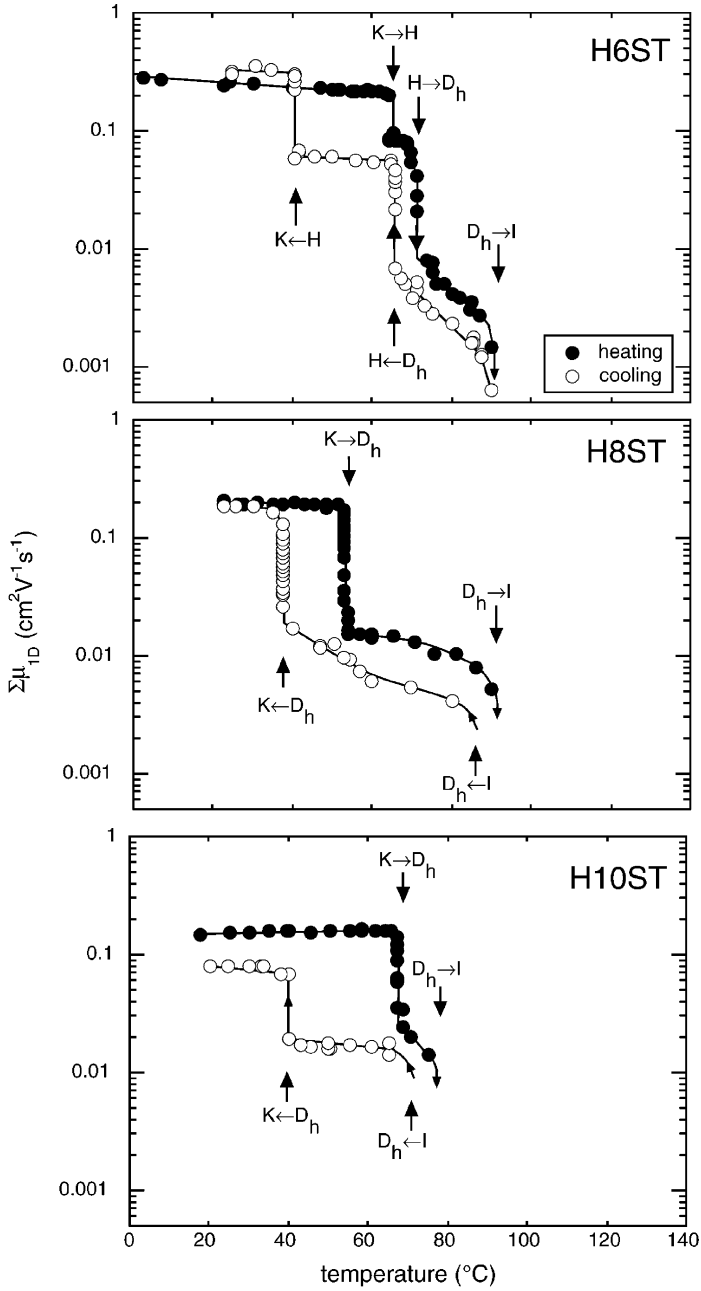

FIGURE 11 The temperature dependences of the intracolumnar charge mobility for hexakis(alkylthio)-triphenylenes on first heating (filled circles) and cooling (open circles). The phase transition temperatures as determined by DSC are indicated by vertical arrows. From reference [2].

TABLE I Intracolumnar Charge Carrier Mobilities ($\Sigma\mu_{1D}$) in the Different Phases of the Triphenylene Compounds Measured on the first Heating

Compound	Temperature(°C)	Phase	$\Sigma\mu_{1D}$ (cm^2/Vs)	Refs.
H4OT	22	K	0.0069	2
	88	D_p	0.025	
H5OT	20	K	0.033	2,43
	77	D_h	0.010	
H6OT	18	K	0.012	2,44,45
	68	D_h	0.002	
H6ST	24	K	0.26	2,13,44,45
	65	H	0.087	
	73	D_h	0.0080	
H8ST	23	K	0.20	2
	60	D_h	0.015	
H10ST	18	K	0.15	2
	70	D_h	0.020	
T2-s10	26	K	0.0055	2,35
	80	D_p	0.0095	
T2-s12	24	K	0.0058	2
	75	D_p	0.014	

The values of $\Sigma\mu_{1D}$ for the columnar phases of the three monomeric alkoxy compounds show a tendency to decrease with increasing alkyl chain length from 0.02 to 0.008 to 0.002 cm^2/Vs in going from butoxy to pentoxy to hexoxy. A similar tendency has been found in TOF measurements on these compounds which show an overall decrease from 0.012 [33] to 0.0008 cm^2/Vs [27]. Interestingly, the TOF mobility value for the hexoxy derivative has gradually increased over the years from a value of 0.0001, [24,25] to 0.0003 [29], to the most recent value of 0.0008 [27]. The most recent value approaches quite closely the PR-TRMC value of 0.002 cm^2/Vs which is as expected if the methods used for homeotropic alignment in the TOF experiments have gradually improved with time. The importance of good columnar alignment in the TOF measurements was illustrated by the factor of almost 2 decrease in mobility found on shearing the sample between the electrodes in the work of Yoshido *et al.* [29]

The two triphenylene dimers studied showed almost identical behaviour, as can be seen in Figure 12. As for the monomeric butoxy compound, the mobility increases on going from the freshly precipitated crystalline material to the D_p phase; an effect which is in contrast with the general decrease found for K to D_h transitions. The dimers do however differ from the monomer in that no evidence is found for an abrupt decrease corresponding to a return to the K phase on cooling even down to −100°C. At the highest temperatures, the mobility of 0.011 cm^2/Vs found for the

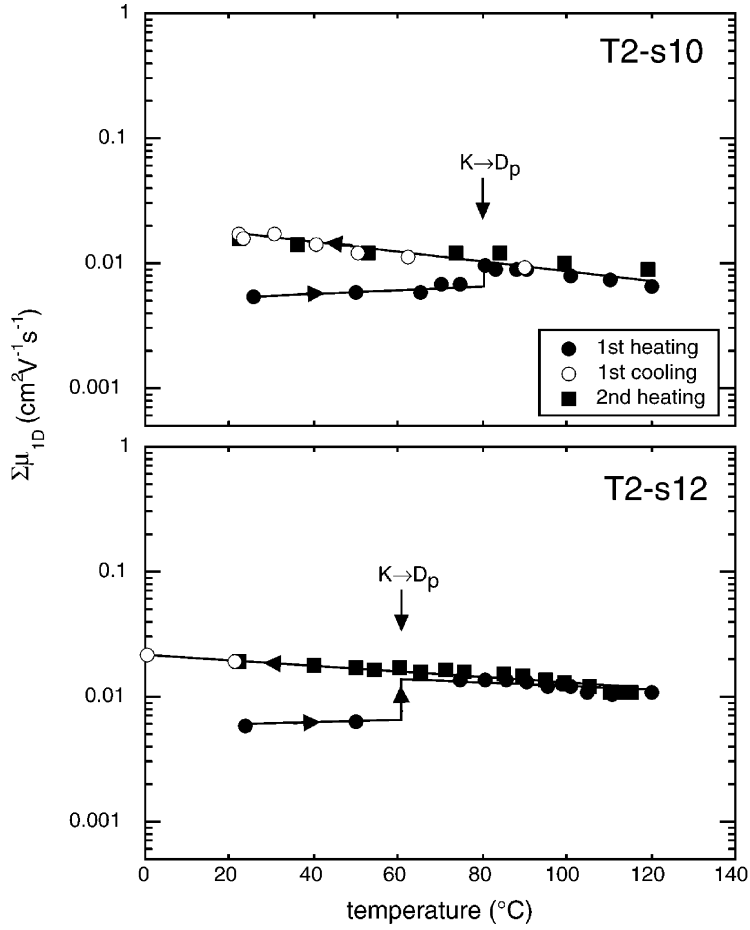

FIGURE 12 The temperature dependences of the intracolumnar charge mobility for the decakis(butoxy)-triphenylene dimers on first heating (filled circles), cooling (open circles), and second heating (filled squares). The phase transition temperatures as determined by DSC are indicated by vertical arrows. From reference [2].

decoxy-bridged dimer using PR-TRMC is the same as that determined by the TOF method [35]. As the material is cooled however the TOF values show an increasing negative deviation from the microwave results with μ_{TOF} two orders of magnitude lower at $-100°\mathrm{C}$. This has been attributed to shallow trapping of holes resulting from static structural disorder in the supercooled plastic mesophase. Different theoretical models have been invoked in an attempt to explain the difference between the DC and

high-frequency microwave measurements [35]. The best description of the data was obtained for a model based on over-the-barrier hopping of charge carriers with an exponential distribution of barrier heights.

A further interesting aspect of the results for the triphenylene compounds is indicated by the large number of experimental points in Figure 11 taken at K to D phase transition temperatures. These points were taken several minutes apart while holding the temperature constant. They demonstrate therefore that the molecular rearrangement accompanying the phase change is a relatively slow process. Great care should therefore be taken when interpreting results of measurements in which the temperature is automatically raised or lowered at a constant rate, as for example in DSC measurements, since full equilibration at close to the transition temperatures may not have occurred.

Phthalocyanines

Peripherally octakis-substituted phthalocyanines, the molecular structures of which are shown in Figure 13, form by far the largest body of compounds studied using the PR-TRMC technique for a given aromatic core. The $\Sigma\mu_{1D}$

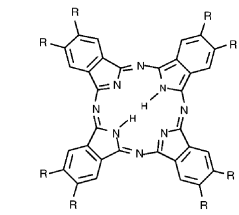

• MPc(SCn)8 : R = SC_nH_{2n+1} with n = 8,12,16 for M = H_2 with n = 8 for M = Cu

• Pc(PhOCn)8 : R = 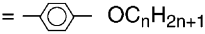 OC_nH_{2n+1} with n = 12,18

• Pc(Ph(OC12)2)8 : R = 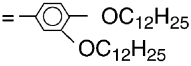

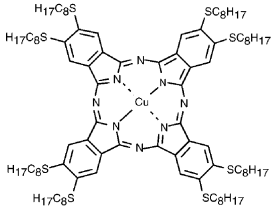

CuPc(SC8)8

• Pc(OCn)8 : R = OC_nH_{2n+1} with n = 6,8,9,11,12,18

• Pc(OC8,2)8 : R = 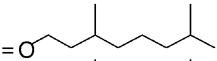

• Pc(OC8,2*)8 : R = 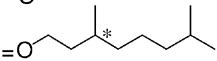

• Pc(OC12,3)8 : R = 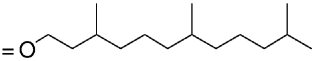

• [Si(Pc(OC8)8)]n : polysiloxane phthalocyanine polymer with R = OC_8H_{17}

FIGURE 13 The molecular structures and pseudonyms of the discotic phthalocyanine derivatives investigated.

TABLE II Phase transition temperatures and intramolecular charge mobilities ($\Sigma\mu_{1D}$) in a variety of peripherally substituted phthalocyanines.

	Transition temperatures (°C)			$\Sigma\mu_{1D}$ (cm^2/Vs)			
Compound	K > D	D > K	D < > I	K phase RT	D phase ($T_{K>D}$+10)	D phase T ≈ 200°C	Refs.
Pc(OC6)8	119	86	> 350	0.20	0.06	0.06	1,3
Pc(OC8)8	94	77	> 350	0.33	0.08	–	1,3
Pc(OC9)8	101	71	> 350	0.30	0.08	0.05	1,3
Pc(OC11)8	83	66	334	0.27	0.07	–	1,3
Pc(OC12)8	91	65	309	0.27	0.05	0.06	1,3
Pc(OC18)8	98	65	247	0.20	0.07	0.05	1,3
Pc(OC6,1)8	158	–	255	0.17	0.19	0.18	1,3
Pc(OC8,2)8	70	a	295	0.37	0.07	0.07	1,3
Pc(OC8,2*)8	b	b	295	b	0.03	0.06	1,3
Pc(OC12,3)8	b	b	185	b	0.04	0.04	1,3
Pc(SC8)8	68	a	> 300	0.55	0.16	0.24	2
CuPc(SC8)8	77	a	> 300	0.54	0.27	0.39	2
Pc(SC12)8	77	a	286	0.26	0.22	0.28	2,45
Pc(SC16)8	95	a	228	0.14	0.12	0.15	2
Pc(PhOC12)8	120	a	261	0.33	0.18	0.19	2,45
Pc(PhOC18)8	78	a	253	0.67	0.24	0.24	2
Pc([PhOC12]2)8	b	b	187	b	0.21	0.24	2
Pc(C10)8	163	155	282	0.13	0.15	0.12	1,3
Pc(COC12)8	78	55	260	0.14	0.04	0.08	1,3
[SiOPc(OC8)8]n	b	b	–	b	0.06	0.09	1,10

a) no recrystallization observed on cooling.
b) no crystalline solid phase formed.

values for different phases of most of the compounds of this class that have been studied are compiled in Table II.

As mentioned in the introduction, the earliest measurements were carried out on the *n*-alkoxy derivatives with the main interest at that time in the kinetics of intercolumnar charge recombination rather than intra-columnar charge transport. In contrast to the dramatic change, by orders of magnitude, in the lifetime of the mobile charge carriers with increasing alkyl chain length, the radiation-induced end-of-pulse conductivity, shown in Figure 2, is seen to be almost identical in magnitude for alkyl chain lengths varying from 6 to 18 with only slight differences in the form of the temperature dependence. In all cases the conductivity was found to return to the initial value on cooling after the first heating run with a hysteresis of approximately 25°. The average room temperature value of the mobility in the K-phase of the *n*-alkoxy-Pc's of 0.26 cm^2/Vs is an order of magnitude larger than for the alkoxy-triphenylene derivatives. A

substantially higher value of $0.067\,cm^2/Vs$ is also found in the D_h phase. Clearly the structural order and/or the electronic interaction within the stacked phthalocyanine cores is much more favourable for charge transport than for stacked triphenylenes, as would be expected on the basis of the much more extensive π-system of the former. Only a weak dependence of the mobility on temperature is found for both the K and D_h phases.

In contrast to the *n*-alkoxy derivatives, the behaviour of derivatives with other chain-to-core coupling elements is quite complex. This is illustrated for the alkylthio compounds in Figure 14. While the mobility values found in the mesophase of these compounds is almost independent of alkyl chain length and equal to *ca* $0.2\,cm^2/Vs$ (substantially higher than for the alkoxy derivatives), the value of $\Sigma\mu_{1D}$ for the freshly precipitated materials is seen to decrease considerably with increasing alkyl chain length. The net result is that the significant decrease, by a factor of approximately 4, found at the phase transition temperature of the octylthio compound on the first heating run is reduced to only approximately 20% for the hexadecylthio derivative. An indication of the underlying reason for this difference is to be found in the fact that on cooling the alkylthio compounds the mobility does not return to the initial value but continues the gradual decrease found in the high temperature D_h phase. We conclude that on precipitation the alkylthio compounds have a tendency to form domains some of which have a tilted crystalline, K-phase, structure and others a columnar D_h structure, with the tendency towards the latter increasing with increasing length of the alkyl chains. This is a rather important conclusion since liquid crystallinity at room temperature could be a favourable property for applications in device structures.

This propensity for the formation of a stable room-temperature D_h phase, either on cooling after heating above the K to D transition temperature or directly on precipitation, has been found to be induced by other structural modifications. For example, this is the case for peripheral octyloxyphenyl substituents as shown in Figure 15. Methyl substitution in the *n*-alkyl chains also results in room temperature liquid crystallinity for 3,7-dimethyloctyloxy and 3,7,11-trimethyldodecyloxy substituents. The latter compound is particularly interesting since, not only is it liquid crystalline at all temperatures, it also has a clearing temperature below 200°C. This is more than 100 degrees below the clearing temperature for the unsubstituted *n*-alkyl derivatives.

A hexagonal columnar structure has also been found at all temperatures for the polymerised siloxane derivative of octa-octyloxy-phthalocyanine [10]. This is observed in PR-TRMC measurements as a gradual increase in the charge mobility from −100 to +200°C with no indication of an abrupt change at any intervening temperature.

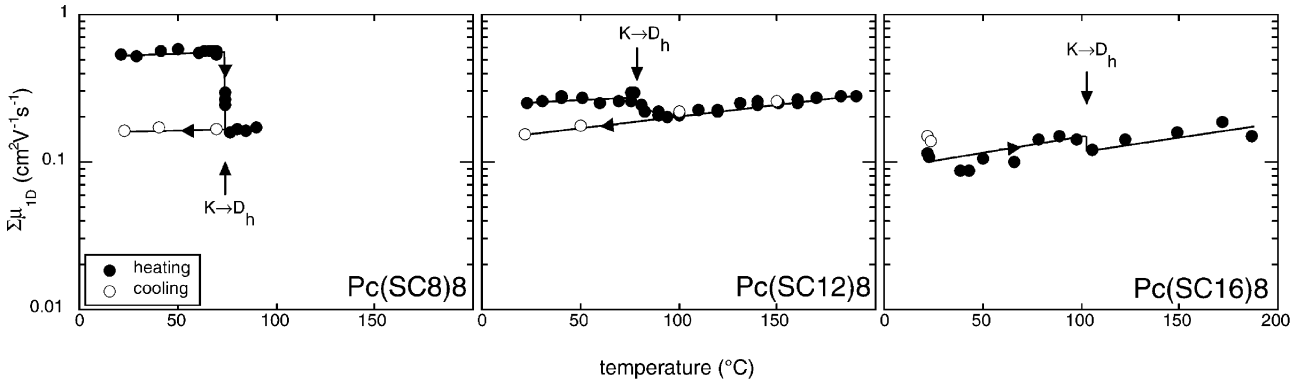

FIGURE 14 The temperature dependences of the intracolumnar charge mobilities determined for the octakis(*n*-alkylthio)-phthalocyanines for the first heating (filled circles) and cooling (open circles) trajectories. The solid to mesophase transition temperatures as determined by DSC on heating are shown by the vertical arrows. From reference [2].

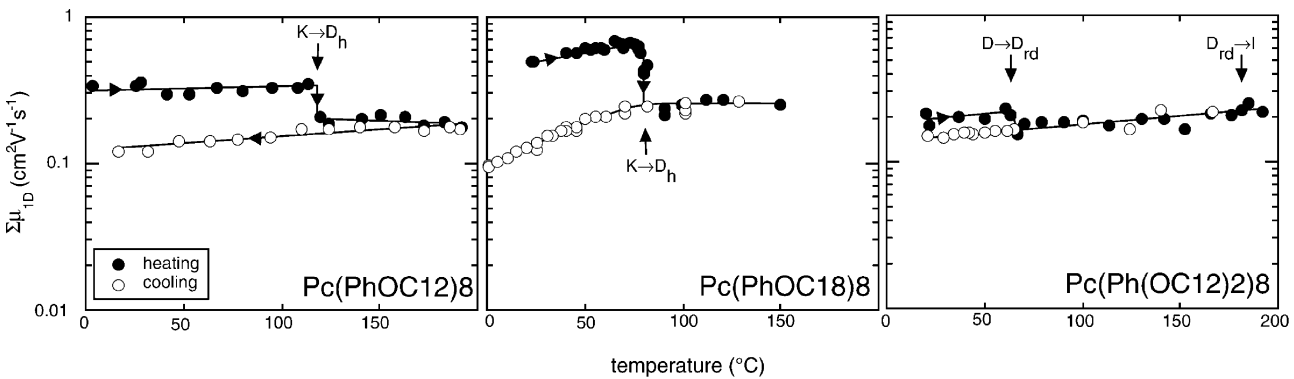

FIGURE 15 The temperature dependences of the intracolumnar charge mobilities determined for the peripherally *n*-alkoxyphenyl-substituted phthalocyanines for the first heating (filled circles) and cooling (open circles) trajectories. The solid to mesophase transition temperatures as determined by DSC on heating are shown by the vertical arrows. From reference [2].

To date no TOF measurements of mobilities have proven possible for discotic phthalocyanine derivatives, mainly because of their very high clearing temperatures. Drift mobilities of 0.9 cm^2/Vs, [36] and 3.2 cm^2/Vs [37], have however been determined for non-peripherally-substituted phthalocyanines. These single crystal values are at most only an order of magnitude larger than the maximum mobility values found for the K-phase of the discotic derivatives measured by PR-TRMC.

Porphyrins

Only a limited number of discotic porphyrin derivatives have been studied using PR-TRMC, the structures of which are given in Figure 16. The mobility values are listed in Table III together with information on their phase transition temperatures. As mentioned in the introduction, these compounds were of considerable importance in the early stage of PR-TRMC studies of discotics since their clearing points were well within the range of the cryostat used. They could therefore be used to demonstrate the dramatic decrease of the charge mobility on going from the columnar

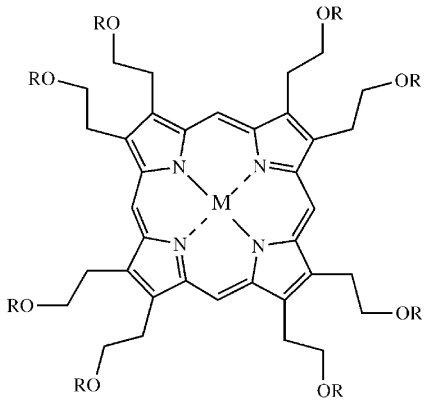

- $H_2PCH_2CH_2OC9$: OR = OC_9H_{19} , M = 2 x H
- $ZnPCH_2CH_2OC9$: OR = OC_9H_{19} , M = Zn
- $H_2PCH_2CH_2OC10$: OR = $OC_{10}H_{21}$, M = 2 x H
- $MPCH_2CH_2OC10$: OR = $OC_{10}H_{21}$, M = Ni, Pd, Cu, Co, Zn

FIGURE 16 The molecular structures and pseudonyms of the octakis(*n*-alkoxyethyl)porphyrins investigated.

TABLE III Phase Transition Temperatures and Intracolumnar Mobilities, $\Sigma\mu_{1D}$, in Discotic Porphyrin Derivatives on Heating

	Transition temperatures (°C)		$\Sigma\mu_{1D}$ (cm^2/Vs)		
compound	K > D	K/D > I	K(RT)	D(106°C)	refs
P(C2OC9)8	a	92	0.20	a	1,9
ZnP(C2OC9)8	99	149	0.26	0.060	1,9
P(C2OC10)8	a	96	0.34	a	1
NiP(C2OC10)8	a	95	0.35	a	1
PdP(C2OC10)8	97	118	0.39	0.056	1
CuP(C2OC10)8	96	129	0.36	0.065	1
CoP(C2OC10)8	95	133	0.27	0.053	1
ZnP(C2OC10)8	95	147	0.30	0.061	1

a) no mesophase formed.

mesophase to the isotropic liquid shown in Figure 3. This confirmed that extensive columnar order was a prerequisite for charge mobilities much higher than that for molecular diffusion.

The porphyrins are also the only series of compounds for which the effect of different central metal atoms on the charge transport properties for a heterocyclic core have been investigated. Both the metal-free and nickel derivatives displayed no mesophase between the crystalline solid and the isotropic liquid. The other four compounds did however show mesomorphic behaviour. Despite expectations to the contrary, no effect of the central metal was found either in the crystalline or liquid crystalline phases with all of the mobility values for the decyloxyethyl derivatives lying within the quite narrow ranges of $0.33 \pm 0.6\,cm^2$/Vs and $0.059 \pm 0.6\,cm^2$/Vs respectively. The mobility in the crystalline materials is comparable with the highest values found for the phthalocyanine derivatives. In the liquid crystalline phase however the mobility for the porphyrins is substantially lower. This can be explained by their smaller π-system hence weaker intracolumnar interactions and greater structural disorder in the columns. This is also reflected in their much lower clearing temperatures than for the phthalocyanines.

It is worth pointing out that both porphyrin and phthalocyanine derivatives are of particular interest for photovoltaic applications because of their extensive optical absorptions in the visible region of the solar spectrum.

Hexabenzocoronenes

A more recently studied series of compounds is based on a hexakis-substituted central core of peri-hexabenzocoronene, illustrated in Figure 17.

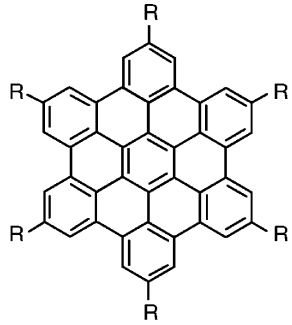

FIGURE 17 The molecular structures and pseudonyms of the hexakis-*peri*-benzocoronene derivatives investigated.

Data for the first heating and cooling runs for these compounds are shown in Figure 18 and the values at temperatures corresponding to different phases are listed in Table IV. For the *n*-alkyl derivatives a behaviour very similar to that found for the *n*-alkoxy phthalocyanines is observed: an abrupt decrease in $\Sigma\mu_{1D}$ at the K to D_h transition temperature and a return to the K-phase value on cooling with a hysteresis of approximately 20°. Both the room temperature K-phase values (in the range 0.4 to 1.0 cm^2/Vs) and the mesophase values (close to 0.3 cm^2/Vs) are however substantially larger than the maximum values found for phthalocyanines.

Based on the phthalocyanine results, it was thought that the use of a paraphenylene chain-to-core coupling element might increase the temperature range of the mesophase. That this was indeed the case is shown by the first heating and cooling runs for the dodecylphenyl derivative of hexabenzocoronene in Figure 18 which display no indication of an abrupt change indicative of a transition to a higher mobility K-phase, even down to −80°C. Even the freshly precipitated material would appear to adopt immediately a hexagonal columnar liquid crystalline structure, which was not the case for the alkoxyphenyl-phthalocyanine compound investigated.

Discotic hexabenzocoronene derivatives are presently undergoing investigation as the electron donating component in blends with electron affinic compounds for applications in photovoltaics. The initial results using the alkoxyphenyl derivative together with a perylene diimide as acceptor have been promising [38].

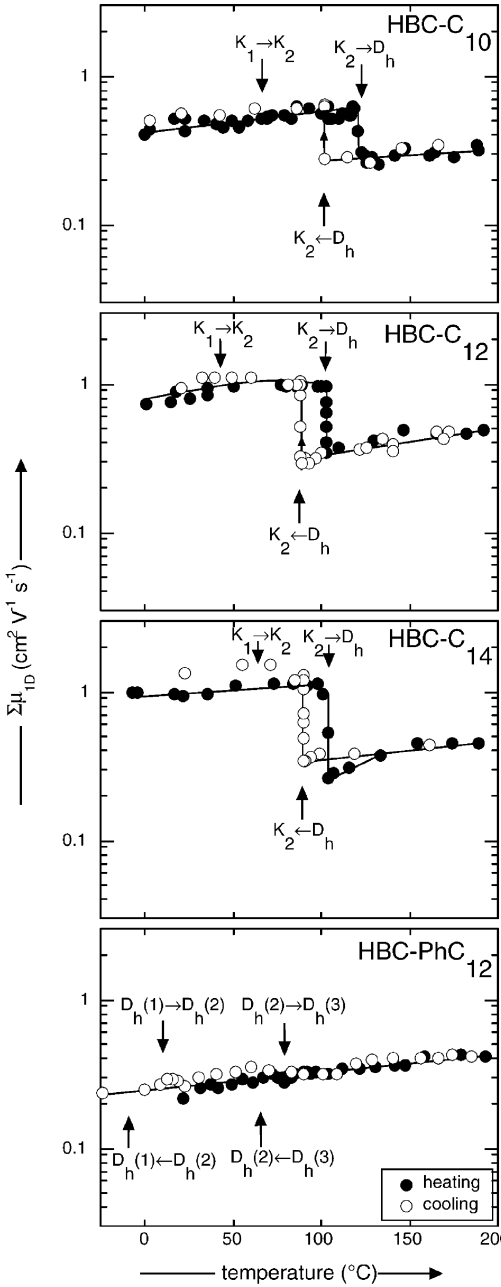

FIGURE 18 The temperature dependences of the intracolumnar charge mobilities determined for the hexakis-*peri*-benzocoronene derivatives for the first heating (filled circles) and cooling (open circles) trajectories. The various phase transition temperatures indicated by DSC are shown by the vertical arrows. From reference [2].

TABLE IV Intracolumnar Charge Carrier Mobilities, $\Sigma\mu_{1D}$, in the Crystalline Phase at Room Temperature and the Columnar Liquid Crystalline Phase at *ca* 120°C for the hexa-*peri*-benzocoronenes on Heating

	$\Sigma\mu_{1D}$ (cm^2/Vs)		
Compound	RT	*ca* 120°C	Refs
HBC-C10	0.46	0.26	2,46
HBC-C12	0.90	0.38	2,45,46
HBC-C14	1.00	0.31	2,46
HBC-PhC12	0.22[a]	0.35	2,45,46

[a]columnar hexagonal phase.

General conclusions

In addition to temperature, which the present results clearly demonstrate is a vital parameter, as expected based on other physical measurement techniques, even small changes in the primary molecular structure of discotic molecules have been shown in the preceding sections to be capable of having a dramatic influence on the mesomorphic and conductive properties of the bulk materials. For technical applications important properties are the range of the liquid crystalline phase (in particular its stability at room temperature and below), the clearing point (for ease of processing), the chemical stability (for durability), the optical absorption spectrum (for solar energy conversion), and last but not least the one-dimensional charge mobility (for applications in light-emitting diodes, field-effect transistors, and photovoltaic cells). In the present work we have shown that mobility values approaching those of *ca* 1 cm^2/Vs found for electrons and holes in organic single crystals [39] are possible even in the columnar mesophases of discotic materials. We discuss very briefly below some (tentative) conclusions that we have been able to reach on the influence of various factors on the mobility based on the PR-TRMC results obtained so far.

The nature of the central metal atom in heterocyclic discotics can influence the mesomorphic properties, as evidenced by the present results on metallo-porphyrin derivatives. However, no significant influence on the charge transport properties is apparent, indicating that charge migration must occur primarily via interactions between neighbouring aromatic (π-systems. The central atom can have a considerable influence on the photophysical properties however, e.g. the optical absorption and emission spectra, and intersystem crossing efficiency. This could be an important consideration in solar energy conversion applications [40].

The nature of the aromatic core itself is obviously crucial to all physical properties. When the charge transport properties obtained to date are compared, it is clear that a larger core results in a higher mobility in the mesophase. An empirical relationship between mobility and core size has recently been proposed by the present authors [41]. This dependence can be understood in terms of a greater stability of the columnar structure for the larger π-systems which results in a decrease in the rotational, longitudinal, and lateral fluctuations in the columnar structure. An increased electronic interaction between cores would also be expected for the larger π-systems. Theoretical studies should be able to determine which is the dominating influence. The fact that the mobilities in the crystalline phases of the compounds studied differ much less than in their mesophases is to be expected since thermally perturbed structural disorder will be greatly reduced in all cases.

The strong influence of the unit coupling the mesogenic alkyl chains to the core was perhaps unexpected. This can apparently completely change the morphological properties, as shown by the comparison between the alkoxy-, alkylthio-, and alkoxyphenyl- phthalocyanines for which a dramatically increased stability of the liquid crystalline phase is achieved. A more subtle influence on the electronic coupling between neighboring core units is however also possible and is indicated by the significantly larger mobilities in alkylthio compared with alkoxy substituted triphenylenes, even in the crystalline solids.

The influence of the structure of the peripheral alkyl chains is of more importance than might have initially been expected. In particular, the effect of branching methyl groups in increasing the stability of the mesophase and lowering the clearing temperature is dramatic for phthalocyanine derivatives. In addition, the possibility of introducing chirality into the overall columnar structure using readily available optically active methyl-branched alkyl substituents could be important in the structural organization of discotic molecules [42].

In conclusion, we have shown that the PR-TRMC technique is not just a tool for measuring the mobility of charge in discotic materials, it is in addition a sensitive method of characterizing the phase behaviour of these materials and the influence of physical and structural parameters thereon.

REFERENCES

[1] Schouten, P. G. (1994). "Charge Carrier Dynamics in Pulse-Irradiated Columnar Aggregates of Mesomorphic Porphyrins and Phthalocyanines", ***PhD thesis***, Delft University of Technology: ISBN 90-73861-22-5.

[2] Van de Craats, A. M. (2000). "Charge Transport in Self-Assembling Discotic Liquid Crystalline Materials" ***PhD thesis***, Delft University Press: ISBN 90-407-2040-1.

[3] Schouten, P. G., Warman, J. M., De Haas, M. P., Van Nostrum, C. F., Gelinck, G. H., Nolte, R. J. M., Copyn, M. J., Zwikker, J. W., Engel, M. K., Hanack, M., Chang, Y. H., & Ford, W. T. (1994). *J. Am. Chem. Soc.* , *116*, 6880.
[4] Schouten, P. G., Warman, J. M., & De Haas, M. P. (1993). *J. Phys. Chem.*, *97*, 9863.
[5] Warman, J. M., De Haas, M. P., Van der Pol, J. F., & Drenth, W. (1989). *Chem. Phys. Lett.*, *164*, 581.
[6] Warman, J. M., De Haas, M. P., Smit, K. J., Paddon-Row, M. N., & Van der Pol., J. F. (1990). *Mol. Cryst. Liq. Cryst.*, *183*, 375.
[7] Schouten, P. G., Warman, J. M., Gelinck, G. H., & Copyn, M. J. (1995). *J. Phys. Chem.*, *99*, 17780.
[8] Warman, J. M., Schouten, P. G., Gelinck, G. H., & De Haas, M. P., (1996). *Chem. Phys.*, *212*, 183.
[9] Schouten, P. G., Warman, J. M., De Haas, M. P., Fox, M-A., & Pan, H-L. (1991). *Nature*, *353*, 736.
[10] Schouten, P. G., Warman, J. M., De Haas, M. P., Van der Pol, J. F., & Zwikker, J. W. (1992). *J. Am. Chem. Soc.*, *114*, 9028.
[11] Adam, D., Closs, F., Frey, T., Funhoff, D., Haarer, D., Ringsdorf, H., Schuhmacher, P., & Siemensmeyer, K. (1993). *Phys. Rev. Lett.*, *70*, 457.
[12] Adam, D., Haarer, D., Closs, F., Frey, T., Funhoff, D., Siemensmeyer, K., Schuhmacher, P., & Ringsdorf, H. (1993). *Ber. Bunsenges. Phys. Chem.*, *97*, 1366.
[13] Van de Craats, A. M., Warman, J. M., De Haas, M. P., Adam, D., Simmerer, J., Haarer, D.,& Schuhmacher, P. (1996). *Adv. Mater.*, *8*, 823.
[14] Alig, R., Bloom, S., & Struck, C. W. (1980). *Phys. Rev. B*, *22*, 5565.
[15] Infelta, P. P., De Haas, M. P., & Warman, J. M. (1977). *Radiat. Phys. Chem.*, *10*, 353.
[16] Warman, J. M. & De Haas., M. P. (1991). *Pulse Radiolysis*, In: Chapt. 6, Tabata,Y. (Ed.)., CRC Press Inc.: Boca Raton.
[17] Hummel, A. (1992) In: *The Chemistry of Alkanes and Cycloalkanes*, John Wiley & Sons: New York, 743–780.
[18] Schmidt, W. F. & Allen, A. O. (1968). *J. Phys. Chem.* , *72*, 3730.
[19] Warman, J. M. (1982). In: *The Study of Fast Processes and Transient Species by Electron Pulse Radiolysis*, Baxendale, J. H. & Busi, F. (Eds.)., Reidel: Dordrecht, 129–161.
[20] Warman, J. M., Asmus, K-D., & Schuler, R. H. (1969). *J. Phys. Chem.*, *73*, 931.
[21] Adam, D., Schuhmacher, P., Simmerer, J., Häussling, L., Siemensmeyer, K., Etzbach, K. H., Ringsdorf, H., & Haarer, D. (1994). *Nature*, *371*, 141.
[22] Arikainen, E. O., Boden, N., Bushby, R. J., Clements, J., Movaghar, B., & Wood, A. (1995). *J. Mater. Chem.*, *5*, 2161.
[23] Bengs, H., Closs, F., Frey, T., Funhoff, D., Ringsdorf, H., & Siemensmeyer, K. (1993). *Liq. Cryst.*, *15*, 565.
[24] Boden, N., Bushby, R. J., Cammidge, A. N., Clements, J., Luo, R., & Donovan, K. J. (1995). *Mol. Cryst. Liq. Cryst.*, *261*, 251.
[25] Boden, N., Bushby, R. J., Clements, J., Movaghar, B., Donovan, K. J., & Kreouzis, T. (1995). *Phys. Rev. B.*, *52*, 13274.
[26] Boden, N., Bushby, R. J., Clements, J., Donovan, K., Movaghar, B., & Kreouzis, T. (1998). *Phys. Rev. B*, *58*, 3063.
[27] Kreouzis, T., Donovan, K. J., Boden, N., Bushby, R. J., Lozman, O. R., & Liu, Q. (2001). *J. Chem. Phys.*, *114*, 1797.
[28] Ochse, A., Kettner, A., Kopitzke, J., Wendorff, J. H., & Bässler, H. (1999). *Phys. Chem. Chem. Phys.*, *1*, 1757.
[29] Yoshido, K., Nakayama, H., Ozaki, M., Onoda, M., & Hamaguchi, M. (1997). *Jpn. J. Appl. Phys.*, *36*, 5183.

[30] Chandrasekhar, S., Sadashiva, B. K., & Suresh, K. A. (1977). *Pramana*, *9*, 471.
[31] Glüsen, B., Heitz, W., Kettner, A., & Wendorff, J. B. (1996). *Liq. Cryst.*, *20*, 627.
[32] Kranig, W., Boeffel, C., & Spiess, H. W. (1990). *Macromolecules*, *23*, 4061.
[33] Simmerer, J., Glüsen, B., Paulus, W., Kettner, A., Schuhmacher, P., Adam, D., Etzbach, K-H., Siemensmeyer, K., Wendorff, J. H., Ringsdorf, H., & Haarer, D. (1996). *Adv. Mater.*, *8*, 815.
[34] Zamir, S., Poupko, R., Luz, Z., Huser, B., Boeffel, C., & Zimmermann, H. (1994). *J. Am. Chem. Soc.*, *116*, 1973.
[35] Van de Craats, A. M., Siebbeles, L. D. A., Bleyl, I., Haarer, D., Berlin, Y. A., Zharikov, A. A., & Warman, J. M. (1998). *J. Phys. Chem. B*, *102*, 9625.
[36] Usov, N. N. & Benderskii, V. A. (1970). *Phys. Stat. Solidi.*, *B37*, 535.
[37] Cox, G. A. & Knight, P. C. (1974). *J. Phys. C: Solid State Phys.*, *7*, 146.
[38] Schmidt-Mende, L., Fechtenkotter, A., Mullen, K., Moons, E., Friend, R. H., & Mackenzie, J. D. (2001). *Science*, *293*, 1119.
[39] Schein, L. B. (1977). *Phys. Rev.* , *B15*, 1024.
[40] Kroeze, J. E., Savenije, T. J., & Warman, J. M. (2002). *Adv. Mater.*, *14*, 1760.
[41] Van de Craats, A. M., & Warman, J. M. (2001). *Adv. Mater.*, *13*, 130.
[42] Van Nostrum, C. F., Bosman, A. W., Gelinck, G. H., Picken, S. J., Schouten, P. G., Warman, J. M., Schouten, A-J., & Nolte, R. J. M. (1993). *J. Chem. Soc., Chem. Commun.*, *14*, 1120.
[43] Warman, J. M., & Schouten, P. G. (1995). *J. Phys. Chem.*, *99*, 17181.
[44] Van de Craats, A. M., De Haas, M. P., & Warman, J. M. (1996). *Synth. Met.*, *86*, 2125.
[45] Van de Craats, A. M. & Warman, J. M. (2001). *Synth. Met.*, *121*, 1287.
[46] Van de Craats, A. M., Warman, J. M., Fechtenkötter, A., Brand, J. D., Harbison, M. A., & Müllen, K. (1999). *Adv. Mater.*, *11*, 1469.